J. Fluid Mech. (1999), *vol.* 387, *pp.* 255–269. Printed in the United Kingdom

Resonant scattering of edge waves by longshore periodic topography: finite beach slope

By YONGZE CHEN AND R. T. GUZA

Center for Coastal Studies, Scripps Institution of Oceanography, La Jolla, CA 92093, USA

(Received 26 May 1998 and in revised form 2 November 1998)

The resonant scattering of low-mode progressive edge waves by small-amplitude longshore periodic depth perturbations superposed on a plane beach has recently been investigated using the shallow water equations (Chen & Guza 1998). Coupled evolution equations describing the variations of edge wave amplitudes over a finite-size patch of undulating bathymetry were developed. Here similar evolution equations are derived using the full linear equations, removing the shallow water restriction of small $(2N + 1)\theta$, where N is the maximum mode number considered and θ is the unperturbed planar beach slope angle. The present results confirm the shallow water solutions for vanishingly small $(2N + 1)\theta$ and allow simple corrections to the shallow water results for small but finite $(2N + 1)\theta$. Additionally, multi-wave scattering cases occurring only when $(2N + 1)\theta = O(1)$ are identified, and detailed descriptions are given for the case involving modes 0, 1, and 2 that occurs only on a steep beach with $\theta = \pi/12$.

1. Introduction

The resonant scattering of low-mode progressive edge waves by small-amplitude longshore periodic depth perturbations superposed on a gently sloping planar beach was recently investigated using the shallow water equations (Chen & Guza 1998; hereafter referred to as CG). In single-wave scattering, an incident edge wave is resonantly scattered into a single additional progressive edge wave having the same or different mode number (i.e. longshore wavenumber), and propagating in the same or opposite direction (forward and backward scattering, respectively), as the incident edge wave. Backscattering into an edge wave with the same mode number as the incident edge wave, the analogue of Bragg scattering of surface waves (Heathershaw 1982; Mei 1985), is a special case of single-wave backward scattering. In multi-wave scattering, simultaneous forward and backward resonant scattering results in several (rather than only one) new progressive edge waves.

The shallow water equations used by CG require $(2N + 1)\theta \ll 1$, where N is the maximum mode number considered and θ is the beach slope angle in radians. Here this restriction is removed by using the full linear theory. The shallow water results are recovered for vanishingly small $(2N+1)\theta$, and the effect of finite beach slope is shown. Additionally, multi-wave scattering cases occurring only when $(2N + 1)\theta = O(1)$ are investigated. The paper is organized as follows. The basic full theory equations are given in § 2. In § 3, single-wave scattering equations and solutions for the slowly varying amplitudes of the incident and resonantly scattered edge waves are obtained and compared with their counterparts in the shallow water theory. In § 4, full theory equations for multi-wave scattering involving modes 0 and 1 are compared with

previous shallow water results, and a multi-wave scattering case involving modes 0, 1, and 2 at steep beach angle $\theta = \pi/12$ is described. In § 5, finite-slope effects are shown to be small for the examples considered in CG.

2. Basic equations

Cartesian coordinates are used, with the z-axis vertically upwards (the mean sea surface is located at $z = 0$), the x-axis pointing seawards (the mean shoreline is located at $x = z = 0$), and the y-axis parallel to the undisturbed shoreline. The governing equations for three-dimensional linear edge waves propagating over a plane beach (depth variation $h_0(x) = sx$) with superposed small-amplitude, longshore periodic perturbations ($h_1(x, y)$) are

$$\Phi_{xx} + \Phi_{yy} + \Phi_{zz} = 0, \qquad -sx - h_1(x, y) < z < 0, \tag{2.1a}$$

$$\Phi_{tt} + g\Phi_z = 0, \qquad z = 0, \tag{2.1b}$$

$$\Phi_z + s\Phi_x + \Phi_x h_{1x} + \Phi_y h_{1y} = 0, \qquad z = -sx - h_1(x, y), \tag{2.1c}$$

where Φ is the velocity potential, g is gravitational acceleration, and $s = \tan\theta$ is the unperturbed beach slope (θ is the beach slope angle in radians). The ratio of the typical slope of the depth perturbation to the unperturbed beach slope, $\epsilon = O(|\nabla h_1|/s)$, is assumed small and used as the perturbation parameter.

To consider the scattering of a mode-n edge wave propagating in the positive y-direction with (positive) wavenumber k_n and frequency ω over an undulating beach, introduce the slow variables $T = \epsilon t$, $Y = \epsilon y$, and the multiple-scale expansion

$$\Phi = \Phi_0(t, x, y, z, T, Y) + \epsilon\Phi_1(t, x, y, z, T, Y) + O(\epsilon^2). \tag{2.2}$$

The longshore periodic depth perturbation with wavenumber k_t is expressed as

$$h_1 = c_0(x) + \left[c_1(x)\mathrm{e}^{\mathrm{i}k_t y} + *\right], \tag{2.3}$$

where $*$ denotes complex conjugate. Substituting (2.2) into (2.1), replacing h_1 by ϵh_1, and expanding the bottom boundary condition (2.1c) about $z = -sx$ yields equations at $O(\epsilon^0)$

$$\Phi_{0xx} + \Phi_{0yy} + \Phi_{0zz} = 0, \qquad -sx < z < 0, \tag{2.4a}$$

$$\Phi_{0tt} + g\Phi_{0z} = 0, \qquad z = 0, \tag{2.4b}$$

$$\Phi_{0z} + s\Phi_{0x} = 0, \qquad z = -sx, \tag{2.4c}$$

and at $O(\epsilon)$

$$\Phi_{1xx} + \Phi_{1yy} + \Phi_{1zz} = -2\Phi_{0yY}, \qquad -sx < z < 0, \tag{2.5a}$$

$$\Phi_{1tt} + g\Phi_{1z} = -2\Phi_{0tT}, \qquad z = 0, \tag{2.5b}$$

$$\Phi_{1z} + s\Phi_{1x} = (\Phi_{0zz} + s\Phi_{0xz})\, h_1 - \left(\Phi_{0x}h_{1x} + \Phi_{0y}h_{1y}\right), \qquad z = -sx. \tag{2.5c}$$

The wavenumber k_t of the perturbed depth (2.3) satisfies the resonance condition

$$k_t = k_n - k_m, \tag{2.6}$$

where the wavenumbers k_n and k_m of mode-n and mode-m edge waves satisfy the linear edge wave dispersion relation (Ursell 1952)

$$\omega^2 = gk_n \sin(2n + 1)\theta = g|k_m| \sin(2m + 1)\theta \tag{2.7}$$

with $(2j + 1)\theta < \pi/2$ for all allowed mode numbers j.

3. Single-wave scattering

3.1. *Evolution equations and solutions*

Anticipating that interaction between the perturbed bathymetry and the incident mode-n edge wave resonantly excites only a mode-m edge wave (single-wave scattering), write the $O(\epsilon^0)$ solution as

$$\Phi_0 = A_0(T,Y)\phi_n(x,z;k_n)\mathrm{e}^{\mathrm{i}(k_n y-\omega t)} + B_0(T,Y)\phi_m(x,z;|k_m|)\mathrm{e}^{\mathrm{i}(k_m y-\omega t)} + *, \tag{3.1}$$

where the edge wave velocity potentials are given by

$$\begin{aligned}\phi_j(x,z;k_j) = \left[1+2\sum_{i=1}^{j}A_{ij}\right]^{-1}\Bigg\{ &\exp\left[-k_j x\cos\theta + k_j z\sin\theta\right] \\ &+\sum_{i=1}^{j}A_{ij}\big\{\exp\left[-k_j x\cos(2i-1)\theta - k_j z\sin(2i-1)\theta\right] \\ &+\exp\left[-k_j x\cos(2i+1)\theta + k_j z\sin(2i+1)\theta\right]\big\}\Bigg\} \quad (j=m,n),\end{aligned} \tag{3.2}$$

with

$$A_{ij} = (-1)^i\prod_{l=1}^{i}\frac{\tan(j-l+1)\theta}{\tan(j+l)\theta} \tag{3.3}$$

(Ursell 1952). Note that ϕ_j is normalized to unity at the shoreline ($x=z=0$).

Equations for the slowly varying edge wave amplitudes A_0 and B_0 in (3.1), determined from solvability conditions at $O(\epsilon)$, are

$$A_{0T} + C_{gn}A_{0Y} = \mathrm{i}\left[\alpha_n C_{gn}A_0 + r_{mn}^{-1}\beta_{nm}^{\pm}C_{gm}B_0\right], \tag{3.4a}$$

$$B_{0T} \pm C_{gm}B_{0Y} = \mathrm{i}\left[\alpha_m C_{gm}B_0 + r_{mn}(\beta_{nm}^{\pm})^* C_{gn}A_0\right], \tag{3.4b}$$

where

$$C_{gn} = \mathrm{d}\omega/\mathrm{d}k_n = \omega/2k_n, \quad C_{gm} = \mathrm{d}\omega/\mathrm{d}|k_m| = \omega/2|k_m| \tag{3.5}$$

are the group velocity magnitudes of mode-n and mode-m edge waves, $+$ and $-$ signs correspond to forward and backward scattering, respectively, and

$$\alpha_j = \frac{g d_j}{2C_{gj}^2}\int_0^\infty\left\{\left[c_0(\phi_{jx})^b\right]_x - k_j^2 c_0\phi_j^b\right\}\phi_j^b\mathrm{d}x, \quad d_j = \cos(2j+1)\theta \quad (j=n,m), \tag{3.6}$$

$$r_{mn} = (d_m/d_n)^{1/2}, \tag{3.7}$$

$$\beta_{nm}^{\pm} = \frac{g(d_n d_m)^{1/2}}{2C_{gm}C_{gn}}\left\{\frac{\omega^2}{gs}c_1(0) - \int_0^\infty c_1\left[(\phi_{mx})^b(\phi_{nx})^b\sec^2\theta \pm |k_m||k_n|\phi_m^b\phi_n^b\right]\right\}\mathrm{d}x. \tag{3.8}$$

The superscript b indicates that the corresponding function is evaluated at the sea floor $z=-sx$. The full theory evolution equations (3.4) have the same structure as their counterparts (2.16CG) derived from the shallow water equations (hereafter an equation number followed by CG refers to the corresponding equation in Chen & Guza 1998). The full theory formulas for the coefficients α_j (3.6) and $\beta_{nm}^{\pm}$ (3.8) are also similar to their shallow water analogues (2.18CG) and (2.19CG), respectively. Conservation of the total edge wave energy during single-wave scattering follows from (3.4), yielding

$$(E_n+E_m)_T + \left(C_{gn}E_n \pm C_{gm}E_m\right)_Y = 0, \tag{3.9}$$

where

$$E_n = \rho|A_0|^2 \tan(2n+1)\theta, \quad E_m = \rho|B_0|^2 \tan(2m+1)\theta \tag{3.10}$$

are the edge wave energies (per unit longshore length) for mode n and m.

Full theory solutions for single-wave backward and forward scattering (3.4) over a finite-length longshore periodic depth perturbation spanning $0 \leqslant Y \leqslant L$ are now discussed. The incident edge wave is allowed a slight frequency difference (i.e. detuning) $\epsilon\Omega$ from the resonant frequency ω and a corresponding wavenumber detuning $\epsilon\Omega/C_{gn}$ from the resonant wavenumber k_n, where Ω/ω is $O(1)$.

With single-wave backscattering the amplitude variation over the undulating region is written as

$$A_0 = \frac{a_0 g}{2\mathrm{i}\omega} T(Y) \mathrm{e}^{\mathrm{i}[(\alpha_n - \alpha_m + \Omega/C_{gn} - \Omega/C_{gm})Y/2 - \Omega T]}, \quad 0 \leqslant Y \leqslant L, \tag{3.11a}$$

$$B_0 = \frac{a_0 g}{2\mathrm{i}\omega} r_{mn}(C_{gn}/C_{gm}) S(Y) \mathrm{e}^{\mathrm{i}[(\alpha_n - \alpha_m + \Omega/C_{gn} - \Omega/C_{gm})Y/2 - \Omega T]}, \quad 0 \leqslant Y \leqslant L, \tag{3.11b}$$

where a_0 is the incident wave amplitude, and $|T|$ and $|S|$ are transmission and scattering coefficients, respectively. Substitution of (3.11) into (3.4) with the $-$ sign yields evolution equations for T and S that are identical to the shallow water versions. The character of the backscatter solutions (i.e. exponential or oscillatory spatial variation of T and S) depends on whether the magnitude of the total effective detuning wavenumber

$$K = \left(\alpha_n + \alpha_m + \Omega/C_{gn} + \Omega/C_{gm}\right)/2 \tag{3.12}$$

is less than, equal to, or greater than the critical (or cutoff) wavenumber $|\beta_{nm}^-|$ (see (3.7CG)–(3.8CG), (3.11CG), and (3.13CG)–(3.14CG)). Forward scattered and transmitted edge wave amplitudes, written as

$$A_0 = \frac{a_0 g}{2\mathrm{i}\omega} T(Y) \mathrm{e}^{\mathrm{i}[(\alpha_n + \alpha_m + \Omega/C_{gn} + \Omega/C_{gm})Y/2 - \Omega T]}, \quad 0 \leqslant Y \leqslant L, \tag{3.13a}$$

$$B_0 = \frac{a_0 g}{2\mathrm{i}\omega} r_{mn}(C_{gn}/C_{gm}) S(Y) \mathrm{e}^{\mathrm{i}[(\alpha_n + \alpha_m + \Omega/C_{gn} + \Omega/C_{gm})Y/2 - \Omega T]}, \quad 0 \leqslant Y \leqslant L, \tag{3.13b}$$

are oscillatory over the corrugated region irrespective of the detuning magnitude, and solutions for T and S in (3.13) are again identical to their shallow water counterparts (3.28GC)–(3.30CG).

Given equal detuning wavenumbers K and scattering coefficients $\beta_{nm}^{\pm}$, the single-wave backward and forward scattering solutions for T and S over the same undulating bathymetry are identical in the full and shallow water theories. However, the solutions differ because K and $\beta_{nm}^{\pm}$ in the full and shallow water theories are generally not equal.

3.2. *Comparison with shallow water theory for small beach slope*

Evolution equations and solutions for single-wave scattering based on the full theory are expanded for small beach angle $\theta = O(\epsilon^{1/2}/(2N+1))$ and compared with their shallow water counterparts to show the effect of finite beach slope.

For a given topographic wavenumber k_t, the full theory resonant frequency and wavenumbers (ω^f, k_n^f, and k_m^f) are found from the resonance condition (2.6) and the full edge wave dispersion relation (2.7). The corresponding shallow water resonant frequency and wavenumbers (ω^s, k_n^s, and k_m^s) also satisfy (2.6) but the dispersion relation is

$$(\omega^s)^2 = g(2n+1)k_n^s \tan\theta = g(2m+1)|k_m^s| \tan\theta. \tag{3.14}$$

For small $(2N+1)\theta$ the relationships between the resonant frequencies and wavenumbers in the full and shallow water theories are

$$\omega^s = \omega^f \left\{1 + \epsilon\Delta\Omega^{\pm}/\omega^f + O(\epsilon^2)\right\}, \quad \Delta\Omega^{\pm} = \omega^f [2 \mp (2n+1)(2m+1)]\hat{\theta}^2/12, \quad (3.15a)$$

$$k_n^s = k_n^f \left\{1 - \epsilon(2n+1)\left[(2n+1) \pm (2m+1)\right]\hat{\theta}^2/6 + O(\epsilon^2)\right\}, \quad (3.15b)$$

$$|k_m^s| = |k_m^f| \left\{1 - \epsilon(2m+1)\left[(2m+1) \pm (2n+1)\right]\hat{\theta}^2/6 \ + O(\epsilon^2)\right\}, \quad (3.15c)$$

where $\theta^2 = \epsilon\hat{\theta}^2$, and signs are vertically ordered, corresponding to single-wave forward and backward scattering, respectively. Note that in the shallow water theory the phases of the incident and scattered edge waves are $(k_n^s y - \omega^s t)$ and $(k_m^s y - \omega^s t)$, respectively, whereas in the full linear theory they are $(k_n^f y - \omega^f t)$ and $(k_m^f y - \omega^f t)$, respectively (see (2.10CG)–(2.11CG) and (3.1)). To facilitate comparison of the full and shallow water theories, (3.15) is used to cast the full theory amplitudes $A_0^f(T, Y)$ and $B_0^f(T, Y)$ as

$$A_0^f = \hat{A}_0^s \exp\left\{-\mathrm{i}k_n^f(2n+1)[(2n+1) \pm (2m+1)]\hat{\theta}^2 Y/6 - \mathrm{i}\Delta\Omega^{\pm}T\right\}, \quad (3.16a)$$

$$B_0^f = \hat{B}_0^s \exp\left\{-\mathrm{i}|k_m^f|(2m+1)[(2n+1) \pm (2m+1)]\hat{\theta}^2 Y/6 - \mathrm{i}\Delta\Omega^{\pm}T\right\}, \quad (3.16b)$$

where $\hat{A}_0^s(T, Y)$ and $\hat{B}_0^s(T, Y)$ are the wave amplitudes associated with shallow water phases $(k_n^s y - \omega^s t)$ and $(k_m^s y - \omega^s t)$, respectively. Substituting (3.16) into the governing equations for A_0^f and B_0^f (3.4), expanding the coefficients about $\theta = 0$, using (3.15), and neglecting higher-order terms yields

$$\hat{A}_{0T}^s + C_{gn}^s \hat{A}_{0Y}^s = \mathrm{i}\left[\left\{\alpha_n^s + k_n^s[2 + (2n+1)^2]\hat{\theta}^2/6\right\} C_{gn}^s \hat{A}_0^s + \beta_{nms}^{\pm} C_{gm}^s \hat{B}_0^s\right], \quad (3.17a)$$

$$\hat{B}_{0T}^s \pm C_{gm}^s \hat{B}_{0Y}^s = \mathrm{i}\left[\left\{\alpha_m^s + |k_m^s|[2 + (2m+1)^2]\hat{\theta}^2/6\right\} C_{gm}^s \hat{B}_0^s + (\beta_{nms}^{\pm})^* C_{gn}^s \hat{A}_0^s\right]. \quad (3.17b)$$

We have used $\alpha_j^f = \alpha_j^s[1 + O(\epsilon)]$ and $\beta_{nmf}^{\pm} = \beta_{nms}^{\pm}[1 + O(\epsilon)]$, as follows from (3.6)–(3.8) and (2.18CG)–(2.19CG) using $\phi_j^b = L_j(2k_j^s x)\mathrm{e}^{-k_j^s x} + O(\theta^2)$ and $(\phi_{jx})^b = \mathrm{d}[L_j(2k_j^s x)\mathrm{e}^{-k_j^s x}]/\mathrm{d}x + O(\theta^2)$ ($L_j(\chi)$ is the Laguerre polynomials of order j and ϕ_j^b is the corresponding full theory velocity potential at the sea floor).

Equations (3.17) are obtained by rewriting the full theory amplitudes in a form appropriate for shallow water (3.16) and expanding for small beach angle $\theta = O(\epsilon^{1/2}/(2N+1))$. Comparison with the shallow water evolution equations (2.16CG) shows that the additional terms proportional to $\hat{\theta}^2$ in (3.17) arise solely from the differences in the dispersion relations that lead to differences in the calculated resonant frequencies and wavenumbers (3.15), and not from the different spatial structures of the velocity potentials or differences in the group velocities. The shallow water evolution equations (2.16CG) can therefore be corrected by replacing α_n^s and α_m^s with

$$\hat{\alpha}_n^s = \alpha_n^s + k_n^s[2 + (2n+1)^2]\hat{\theta}^2/6, \quad \hat{\alpha}_m^s = \alpha_m^s + |k_m^s|[2 + (2m+1)^2]\hat{\theta}^2/6, \quad (3.18)$$

respectively.

The simplicity of the full theory solutions for single-wave scattering allows direct comparison with the corresponding shallow water solutions. Expanding the full solutions A_0^f and B_0^f given by (3.11) and (3.13) for small θ, neglecting $O(\theta^2)$ terms, and writing the results in the form of (3.16) yields

$$\hat{A}_0^s = \frac{a_0 g}{2\mathrm{i}\omega}\hat{T}^s \exp\left\{\mathrm{i}[(\hat{\alpha}_n^s \pm \hat{\alpha}_m^s + \Omega^s/C_{gn}^s \pm \Omega^s/C_{gm}^s)Y/2 - \Omega^s T]\right\}, \quad (3.19a)$$

$$\hat{B}_0^s = \frac{a_0 g}{2i\omega}(C_{gn}^s/C_{gm}^s)\hat{S}^s \exp\left\{i[(\hat{\alpha}_n^s \pm \hat{\alpha}_m^s + \Omega^s/C_{gn}^s \pm \Omega^s/C_{gm}^s)Y/2 - \Omega^s T]\right\}, \quad (3.19b)$$

for $0 \leqslant Y \leqslant L$, where $\Omega^f = \Omega^s + \Delta\Omega^{\pm} + O(\epsilon)$ has been used ($\epsilon\Omega^f$ ($\epsilon\Omega^s$) is the difference between the incident wave frequency and the full theory (shallow water) resonant frequency ω^f (ω^s), and $\epsilon\Delta\Omega^{\pm}$ is the frequency shift from ω^f to ω^s given by (3.15*a*)). $\hat{T}^s$ and $\hat{S}^s$, obtained by expanding the full solutions, are (as expected) solutions of the expanded evolution equations (3.17) under transformation (3.19). $\hat{T}^s$ and $\hat{S}^s$ can also be obtained from the shallow water solutions T^s and S^s (CG) by replacing the effective shallow water detuning wavenumber $K^s = (\alpha_n^s \mp \alpha_m^s + \Omega^s/C_{gn}^s \mp \Omega^s/C_{gm}^s)/2$ with

$$\begin{aligned}\hat{K}^s &= (\hat{\alpha}_n^s \mp \hat{\alpha}_m^s + \Omega^s/C_{gn}^s \mp \Omega^s/C_{gm}^s)/2 = K^s + [2 \mp (2n+1)(2m+1)]\hat{\theta}^2 k_t/12 \\ &= \tfrac{1}{2}\left[\alpha_n^s \mp \alpha_m^s + (\Omega^s + \Delta\Omega^{\pm})/C_{gn}^s \mp (\Omega^s + \Delta\Omega^{\pm})/C_{gm}^s\right]. \end{aligned} \quad (3.20)$$

The effect of finite beach slope on the variation of wave amplitudes and energy fluxes (i.e. of $|T^s|$ and $|S^s|$) can thus be incorporated in the shallow water theory by an additional frequency shift $\epsilon\Delta\Omega^{\pm}$ from ω^s (see (3.20)), yielding a total frequency detuning of $\epsilon(\Omega^s + \Delta\Omega^{\pm})$. This additional frequency detuning, however, cannot accommodate the phase shift in the exponentials in the complete solutions (3.19) corresponding to the correction in α_j^s (3.18), i.e. $\hat{\alpha}_n^s \pm \hat{\alpha}_m^s + \Omega^s/C_{gn}^s \pm \Omega^s/C_{gm}^s \neq \alpha_n^s \pm \alpha_m^s + (\Omega^s + \Delta\Omega^{\pm})/C_{gn}^s \pm (\Omega^s + \Delta\Omega^{\pm})/C_{gm}^s$.

When $(2N+1)\theta = O(\epsilon)$, the difference in the full and shallow dispersion relations is negligible in the present approximation, and the shallow water and full linear theories are equivalent. However, when $(2N+1)\theta = O(\epsilon^{1/2})$, the full and shallow water theories give qualitatively different predictions for single-wave backscattering if the beach angle θ is large enough that the detuning correction in (3.20) changes the effective detuning wavenumber from subcritical (i.e. $|K^s| < |\beta_{nm}^-|$) to supercritical (i.e. $|\hat{K}^s| > |\beta_{nm}^-|$) or vice versa. For example, the shallow water theory predicts that the amplitude variation of the incident and backscattered waves over the undulating region is exponential when the total effective detuning $K^s = 0$, but oscillatory amplitude variation is predicted (i.e. $|\hat{K}^s| > |\beta_{nm}^-|$) by the full linear theory when $K^s = 0$ and $\hat{\theta}^2 = \theta^2/\epsilon > 12|\beta_{nm}^-|/\{[2 + (2n+1)(2m+1)]k_t\}$ (see (3.20)). The dimensional beach slopes corresponding to these changes in the character of the shallow water backscatter solutions are discussed in § 5. In single-wave forward scattering the wave amplitudes are oscillatory regardless of the detuning magnitude, so the finite-slope correction does not qualitatively change the solutions.

4. Multi-wave scattering

The single-wave scattering assumption, that the interaction of the incident and scattered waves with the periodic topography will not excite additional free edge wave(s), is not always satisfied. Multi-wave scattering occurs when $|2k_n - k_m|$ and/or $|2k_m - k_n|$ satisfy the dispersion relation (2.7) for some mode number(s). When the beach angle $\theta = \pi/12 = 15°$, the perturbed bathymetry with wavenumber $k_t = k_0 - k_1 = k_1 + k_2$ simultaneously forward scatters mode pair (0, 1) and backward scatters mode pair (1, 2). The final multi-wave state in this case involves three waves with three different mode numbers: modes 0 and 1 propagating in the same direction and mode 2 in the opposite direction. Note that when $\theta = \pi/12$ only mode-0, mode-1, and mode-2 edge waves exist (since $(2N+1)\theta < \pi/2$) and all three modes are involved in the scattering process. Multi-wave scattering cases involving a high-mode edge wave

($N \geqslant 5$) occurring when $\theta < 7^\circ$ have also been identified. For example, the perturbed bathymetry with wavenumber $k_t = 2k_5 = k_1 - k_5$ at $\theta = 5.802^\circ$ simultaneously backward scatters mode pair (5, 5) and forward scatters mode pair (1, 5), resulting in four waves in the final state: two mode-1 and two mode-5 propagating in both directions. These particular multi-wave scattering cases do not occur in the shallow water theory because $(2N+1)\theta$ is $O(1)$ and there are large differences between the exact (2.7) and shallow water (3.14) edge wave dispersion relations. On the other hand, for small $(2N+1)\theta$ the shallow and full theory dispersion relations are similar, and multi-wave scattering predicted by the shallow water theory is also expected to occur in the full theory. Below, full theory evolution equations are first derived for the multi-wave scattering case involving two different mode numbers (0 and 1) on a gentle slope studied by CG with the shallow water equations; finite-slope corrections to the CG results are obtained. Multi-wave scattering of all three possible modes (0, 1, and 2) at finite beach angle $\theta = \pi/12$ is discussed next. Solutions for the simultaneous scattering of waves with three different modes have not been presented previously.

4.1. *Multi-wave scattering of modes 0 and 1 with small beach slope*

According to the shallow water dispersion relation (3.14), topography with wavenumber $k_t = 2k_1 = k_0 - k_1$ will simultaneously backward scatter the mode pair (1, 1) and forward scatter the mode pair (0, 1), resulting in four wave components (modes 0 and 1 propagating in both directions). For small beach slope, the full theory dispersion relation (2.7) expanded in θ yields

$$k_0 = 3k_1 - 4k_1\theta^2 + O(\theta^4), \tag{4.1}$$

so exact resonance occurs in the shallow water theory but not with finite θ. The lowest-order full theory velocity potential for this case is written as

$$\begin{aligned}\Phi_0 = \phi_0(x,z;k_0)\left[A_0^+(T,Y)\mathrm{e}^{\mathrm{i}(k_0 y-\omega t)} + A_0^-(T,Y)\mathrm{e}^{\mathrm{i}(-k_0 y-\omega t)}\right]\\ +\phi_1(x,z;k_1)\left[B_0^+(T,Y)\mathrm{e}^{\mathrm{i}(k_1 y-\omega t)} + B_0^-(T,Y)\mathrm{e}^{\mathrm{i}(-k_1 y-\omega t)}\right] + *,\end{aligned} \tag{4.2}$$

with the topographic wavenumber $k_t = 2k_1$ (equivalent results are obtained if $k_t = k_0 - k_1$ is instead used to determine the resonant frequency ω). Solvability conditions at $O(\epsilon)$ again yield evolution equations for the lowest-order amplitudes $A_0^\pm$ and $B_0^\pm$:

$$A_{0T}^+ + C_{g0}A_{0Y}^+ = \mathrm{i}[\alpha_0 C_{g0}A_0^+ + r_{10}^{-1}\beta_{01}^+ C_{g1}B_0^+\mathrm{e}^{\mathrm{i}4\hat{\theta}^2 k_1 Y}], \tag{4.3a}$$

$$A_{0T}^- - C_{g0}A_{0Y}^- = \mathrm{i}[\alpha_0 C_{g0}A_0^- + r_{10}^{-1}(\beta_{01}^+)^* C_{g1}B_0^-\mathrm{e}^{-\mathrm{i}4\hat{\theta}^2 k_1 Y}], \tag{4.3b}$$

$$B_{0T}^+ + C_{g1}B_{0Y}^+ = \mathrm{i}[\alpha_1 C_{g1}B_0^+ + r_{10}(\beta_{01}^+)^* C_{g0}A_0^+\mathrm{e}^{-\mathrm{i}4\hat{\theta}^2 k_1 Y} + \beta_{11}^- C_{g1}B_0^-], \tag{4.3c}$$

$$B_{0T}^- - C_{g1}B_{0Y}^- = \mathrm{i}[\alpha_1 C_{g1}B_0^- + r_{10}\beta_{01}^+ C_{g0}A_0^-\mathrm{e}^{\mathrm{i}4\hat{\theta}^2 k_1 Y} + (\beta_{11}^-)^* C_{g1}B_0^+], \tag{4.3d}$$

where as previously $\theta^2 = \epsilon\hat{\theta}^2$. The factor $\mathrm{e}^{\mathrm{i}4\hat{\theta}^2 k_1 Y}$ in (4.3) reflects the $O(\epsilon\hat{\theta}^2)$ difference between k_0 and $3k_1$ (4.1) (the difference is zero in the shallow water theory, so this factor does not appear in (2.24CG)). Energy conservation follows from (4.3).

For multi-wave scattering involving modes 0 and 1 on a gentle beach slope with $\theta = O(\epsilon^{1/2})$, the relations between (ω^s, k_0^s, k_1^s) and (ω^f, k_0^f, k_1^f) with $k_t = 2k_1^f$ are

$$\omega^s = \omega^f[1 + \tfrac{11}{12}\epsilon\hat{\theta}^2 + O(\epsilon^2)], \quad k_0^s = k_0^f[1 + \tfrac{4}{3}\epsilon\hat{\theta}^2 + O(\epsilon^2)], \quad k_1^s = k_1^f = k_t/2, \tag{4.4}$$

which implies that

$$A_{0f}^\pm = \hat{A}_{0s}^\pm \exp[\mathrm{i}\hat{\theta}^2(\pm\tfrac{4}{3}k_0^f Y - \tfrac{11}{12}\omega^f T)], \quad B_{0f}^\pm = \hat{B}_{0s}^\pm \exp(-\tfrac{11}{12}\mathrm{i}\hat{\theta}^2\omega^f T), \tag{4.5}$$

from (4.2) and (2.23CG), where $\hat{A}_{0s}^{\pm}$ and $\hat{B}_{0s}^{\pm}$ are the wave amplitudes associated with shallow water phases. Substituting (4.5) into (4.3) yields

$$\hat{A}_{0T}^{+} + C_{g0}\hat{A}_{0Y}^{+} = \mathrm{i}[(\alpha_0 + k_0\hat{\theta}^2/2)C_{g0}\hat{A}_0^{+} + \beta_{01}^{+}C_{g1}\hat{B}_0^{+}], \tag{4.6a}$$

$$\hat{A}_{0T}^{-} - C_{g0}\hat{A}_{0Y}^{-} = \mathrm{i}[(\alpha_0 + k_0\hat{\theta}^2/2)C_{g0}\hat{A}_0^{-} + (\beta_{01}^{+})^{*}C_{g1}\hat{B}_0^{-}], \tag{4.6b}$$

$$\hat{B}_{0T}^{+} + C_{g1}\hat{B}_{0Y}^{+} = \mathrm{i}[(\alpha_1 + 11k_1\hat{\theta}^2/6)C_{g1}\hat{B}_0^{+} + (\beta_{01}^{+})^{*}C_{g0}\hat{A}_0^{+} + \beta_{11}^{-}C_{g1}\hat{B}_0^{-}], \tag{4.6c}$$

$$\hat{B}_{0T}^{-} - C_{g1}\hat{B}_{0Y}^{-} = \mathrm{i}[(\alpha_1 + 11k_1\hat{\theta}^2/6)C_{g1}\hat{B}_0^{-} + \beta_{01}^{+}C_{g0}\hat{A}_0^{-} + (\beta_{11}^{-})^{*}C_{g1}\hat{B}_0^{+}], \tag{4.6d}$$

where the subscript s has been dropped for brevity. The differences between (4.6) and its shallow water counterpart (2.24CG) are again in the α terms and arise from the different dispersion relations. The shallow water evolution equations (2.24CG) can be corrected by the following simple substitution

$$\alpha_0 \to \alpha_0 + k_0\hat{\theta}^2/2, \quad \alpha_1 \to \alpha_1 + 11k_1\hat{\theta}^2/6. \tag{4.7}$$

In the single-wave scattering case exact resonances are possible in both full and shallow theories, and there is a frequency shift $\epsilon\Delta\Omega^{\pm}$ (3.15a) that can render a detuned resonance in the shallow water theory into an exactly tuned resonance in the full theory for a given beach slope (see (3.20)). In contrast, the multi-wave resonances are not exact at $O(\theta^2)$ in the full theory (see (4.1)), so there is no frequency shift equivalent to the above changes (4.7) in α_0 and α_1.

When $\theta = O(\epsilon)$, the correction in (4.7) is negligible and the shallow water and full linear theories predict identical multi-wave scattering involving modes 0 and 1. If $\theta = O(\epsilon^{1/2})$, then $\hat{\theta}^2 = O(1)$ and the solutions of (4.6) (or equivalently (4.3)) may differ significantly from those of (4.6) with $\hat{\theta}^2 = 0$, i.e. the solutions of (2.24CG). The effect of finite θ on a perfectly tuned (based on the shallow water dispersion relation) mode-0 incident wave propagating over a long extent of beach cusps $\epsilon h_1(x, y) = a_c \mathrm{e}^{-\pi x/\lambda_c}\cos(2\pi y/\lambda_c)$, where a_c and λ_c are the cusp amplitude and wavelength, is shown in terms of normalized energy fluxes in figure 1 (hereafter the energy flux of a mode-i forward (backward) propagating wave normalized by the energy flux of a mode-j incident wave at $Y = 0$ is denoted as $F_{ij}^{+}(Y)$ ($F_{ij}^{-}(Y)$) with the energy given by (3.10)). Typical solutions are shown for $\hat{\theta}^2$ in each of the four regions where the characteristic equation of (4.6) has different types of roots (see CG for details). For the particular shape beach cusps considered here, the roots change character when $k_0|\beta_{01}^{+}\beta_{11}^{-}|^{-1/2}\hat{\theta}^2 = 0.545, 2.486$, and 3.491. The solutions of (4.6) with $k_0|\beta_{01}^{+}\beta_{11}^{-}|^{-1/2}\hat{\theta}^2 > 0.545$ (figure 1b–d), where backscattering is weak and the wave field over the perturbed depth is dominated by the incident mode-0 and the forward scattered mode-1 edge waves, differ significantly from the solutions with $\hat{\theta}^2 = 0$ (i.e. the solutions of (2.24CG)) (figure 1a), where backscattering is nearly complete. For large enough $\hat{\theta}^2$, forward scattering is also suppressed (not shown).

4.2. *Multi-wave scattering at beach angle $\theta = \pi/12$*

When $\theta = \pi/12$, multi-wave resonances involving a mode-0 and a mode-1 edge wave propagating in the same direction and a mode-2 in the opposite direction are exact. The $O(\epsilon^0)$ velocity potential is written as

$$\Phi_0 = A_0(T, Y)\phi_0(x, z; k_0)\mathrm{e}^{\mathrm{i}(\pm k_0 y - \omega t)} + B_0(T, Y)\phi_1(x, z; k_1)\mathrm{e}^{\mathrm{i}(\pm k_1 y - \omega t)} + C_0(T, Y)\phi_2(x, z; k_2)\mathrm{e}^{\mathrm{i}(\mp k_2 y - \omega t)} + *, \tag{4.8}$$

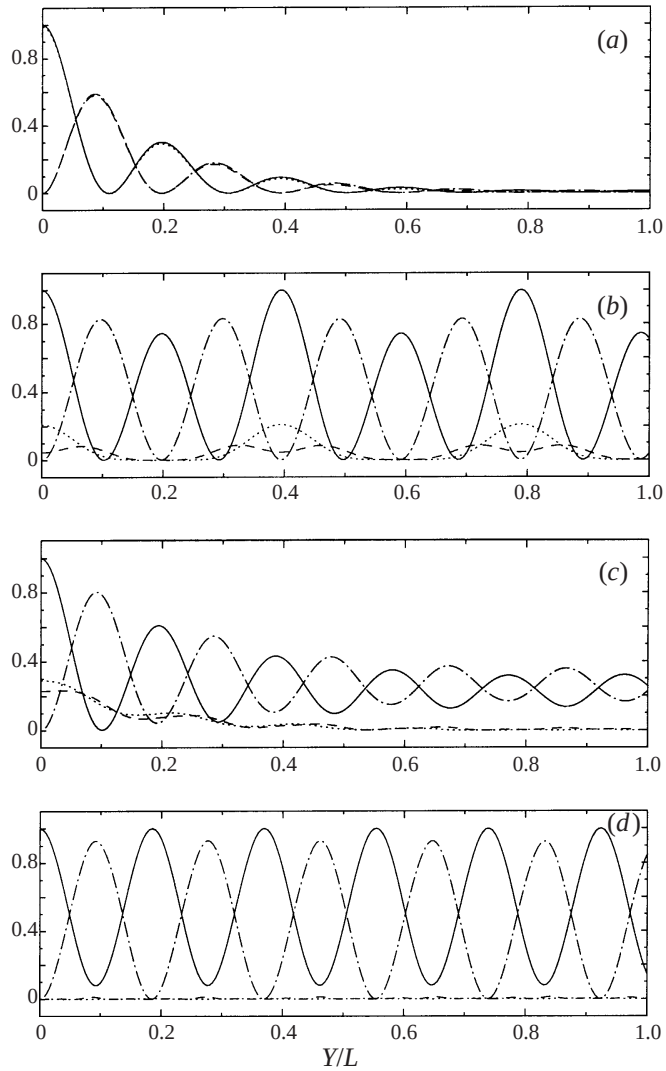

FIGURE 1. Spatial variations of normalized energy fluxes (——, F_{00}^{+}; — · —, F_{10}^{+}; · · · ·, F_{00}^{-}; and - - -, F_{10}^{-}) for multi-wave scattering over beach cusps spanning a fixed length $|\beta_{01}^{+}\beta_{11}^{-}|^{1/2}L = 10.0$, for different beach slopes $\hat{\theta}$, $k_0|\beta_{01}^{+}\beta_{11}^{-}|^{-1/2}\hat{\theta}^2 = 0$ (*a*) (note that $F_{00}^{+} \approx F_{00}^{-}$ and $F_{10}^{+} \approx F_{10}^{-}$), 1.5 (*b*), 3.0 (*c*), and 9.0 (*d*). The detuning vanishes in the shallow water limit ($\hat{\theta} = 0$) and increases as $\hat{\theta}$ increases. The incident wave is mode 0 so boundary conditions are $F_{00}^{+}(0) = 1$ and $F_{10}^{+}(0) = F_{00}^{-}(L) = F_{10}^{-}(L) = 0$.

with the topographic wavenumber $k_t = k_0 - k_1 = k_1 + k_2$, where A_0, B_0, and C_0 are proportional to the amplitudes of mode 0, 1, and 2, respectively; signs are vertically ordered, corresponding to a mode-0 or mode-1 incident wave, and a mode-2 incident wave, respectively. Solvability conditions at $O(\epsilon)$ yield evolution equations for the lowest-order edge wave amplitudes

$$A_{0T} + C_{g0}A_{0Y} = \mathrm{i}\left[\alpha_0 C_{g0}A_0 + r_{10}^{-1}\beta_{01}^{+}C_{g1}B_0\right], \tag{4.9a}$$

$$B_{0T} + C_{g1}B_{0Y} = \mathrm{i}\left[\alpha_1 C_{g1}B_0 + r_{10}(\beta_{01}^{+})^{*}C_{g0}A_0 + r_{21}^{-1}\beta_{12}^{-}C_{g2}C_0\right], \tag{4.9b}$$

$$C_{0T} - C_{g2}C_{0Y} = \mathrm{i}\left[\alpha_2 C_{g2}C_0 + r_{21}(\beta_{12}^{-})^{*}C_{g1}B_0\right], \tag{4.9c}$$

for a mode-0 or mode-1 incident wave, and

$$A_{0T} - C_{g0}A_{0Y} = \mathrm{i}\left[\alpha_0 C_{g0}A_0 + r_{10}^{-1}(\beta_{01}^{+})^{*}C_{g1}B_0\right], \tag{4.10a}$$

$$B_{0T} - C_{g1}B_{0Y} = \mathrm{i}\left[\alpha_1 C_{g1}B_0 + r_{10}\beta_{01}^{+}C_{g0}A_0 + r_{21}^{-1}(\beta_{12}^{-})^{*}C_{g2}C_0\right], \tag{4.10b}$$

$$C_{0T} + C_{g2}C_{0Y} = \mathrm{i}\left[\alpha_2 C_{g2}C_0 + r_{21}\beta_{12}^{-}C_{g1}B_0\right], \tag{4.10c}$$

for a mode-2 incident wave. Coupling occurs between mode-0 and mode-1 edge waves propagating in the same directions and between mode-1 and mode-2 edge waves propagating in opposite directions. No direct coupling occurs between mode-0 and mode-2 edge waves (A_0 and C_0 do not appear in the same equation). Energy conservation follows from (4.9) or (4.10).

For simplicity further assume that the mean (y-averaged) profile does not deviate from the plane beach, i.e. $c_0 = 0$ in (2.3). The general solutions of (4.9) and (4.10) over the undulating region $0 \leqslant Y \leqslant L$ depend on the roots of the characteristic equation

$$(\sigma - \tilde{\alpha}_0)(\sigma - \tilde{\alpha}_1)(\sigma + \tilde{\alpha}_2) + |\beta_{12}^{-}|^2(\sigma - \tilde{\alpha}_0) - |\beta_{01}^{+}|^2(\sigma + \tilde{\alpha}_2) = 0, \tag{4.11}$$

where

$$\tilde{\alpha}_0 = 2k_0\Omega/\omega, \quad \tilde{\alpha}_1 = \tfrac{1}{2}(3^{1/2} - 1)\tilde{\alpha}_0, \quad \tilde{\alpha}_2 = (2 - 3^{1/2})\tilde{\alpha}_0, \tag{4.12}$$

which in turn depend on the frequency detuning of the incident wave Ω. The cubic polynomial characteristic equation (4.11) has three distinct real roots when $0 \leqslant |\Omega| < \Omega_1$, one real and two complex conjugate roots when $\Omega_1 < |\Omega| < \Omega_2$, and three distinct real roots when $|\Omega| > \Omega_2$. When (4.11) has three different roots σ_1, σ_2, and σ_3, the general solutions for (4.9) and (4.10) can be written as

$$\{A_0, B_0, C_0\}^{\mathrm{T}} = \boldsymbol{C}\{\mathrm{e}^{\mathrm{i}\sigma_1 Y}, \mathrm{e}^{\mathrm{i}\sigma_2 Y}, \mathrm{e}^{\mathrm{i}\sigma_3 Y}\}^{\mathrm{T}}\mathrm{e}^{-\mathrm{i}\Omega T}, \tag{4.13}$$

where $\boldsymbol{C}$ is a 3×3 matrix and superscript T denotes matrix transpose. The lengthy expressions for Ω_1, Ω_2, $\sigma_1, \sigma_2, \sigma_3$, and the elements of $\boldsymbol{C}$ are omitted for brevity.

For perfect tuning ($\Omega = 0$), the solution (4.13) to (4.9) and (4.10) simplifies to

$$A_0 = D\left(|\beta_{01}^{+}|^2 \cos RY - |\beta_{12}^{-}|^2 \cos RL\right), \quad B_0 = \mathrm{i}D\frac{C_{g0}}{C_{g1}}r_{10}(\beta_{01}^{+})^{*}R \sin RY, \tag{4.14a,b}$$

$$C_0 = D\frac{C_{g0}}{C_{g2}}r_{20}(\beta_{01}^{+}\beta_{12}^{-})^{*}(\cos RL - \cos RY), \tag{4.14c}$$

for a mode-0 incident wave,

$$A_0 = \mathrm{i}\frac{C_{g1}}{C_{g0}}\frac{\beta_{01}^{+}}{r_{10}R}\left\{|\beta_{01}^{+}|^2 \sin RY + |\beta_{12}^{-}|^2\left[\sin R(L - Y) - \sin RL\right]\right\}, \tag{4.15a}$$

$$B_0 = D\left[|\beta_{01}^{+}|^2 \cos RY - |\beta_{12}^{-}|^2 \cos R(L - Y)\right], \tag{4.15b}$$

$$C_0 = \mathrm{i}\frac{C_{g1}}{C_{g2}}\frac{r_{21}(\beta_{12}^{-})^{*}}{R}\left[|\beta_{01}^{+}|^2(\sin RL - \sin RY) - |\beta_{12}^{-}|^2 \sin R(L - Y)\right], \tag{4.15c}$$

for a mode-1 incident wave, and

$$A_0 = D\frac{C_{g2}}{C_{g0}}\frac{(\beta_{01}^{+}\beta_{12}^{-})^{*}}{r_{20}}\left[\cos R(L - Y) - 1\right], \quad B_0 = \mathrm{i}\frac{C_{g2}}{C_{g1}}\frac{(\beta_{12}^{-})^{*}R}{r_{21}}\sin R(L - Y), \tag{4.16a,b}$$

$$C_0 = D\left[|\beta_{01}^{+}|^2 - |\beta_{12}^{-}|^2 \cos R(L - Y)\right], \tag{4.16c}$$

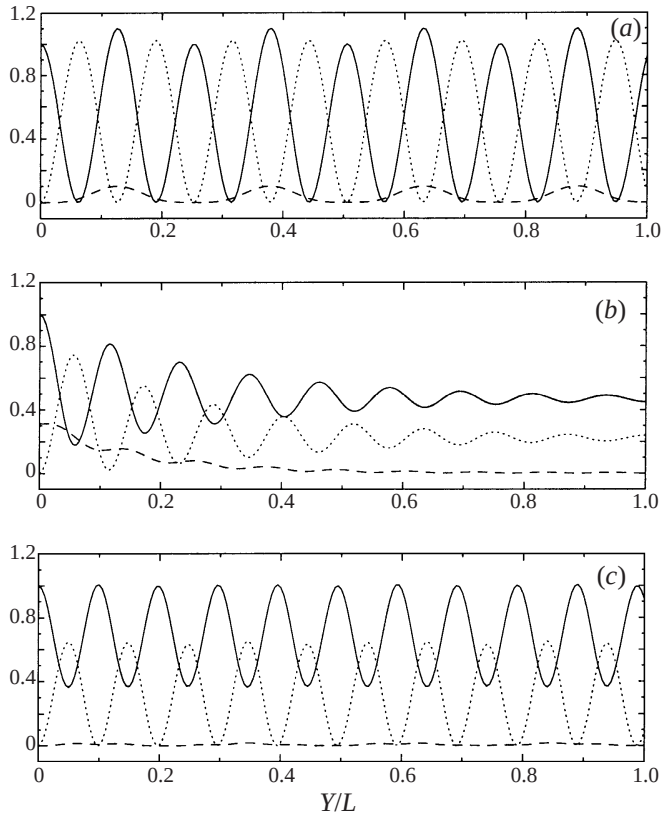

FIGURE 2. Spatial variations of normalized energy fluxes (——, F_{00}^{+}; ····, F_{10}^{+}; and - - -, F_{20}^{-}) for multi-wave scattering at $\theta = \pi/12$ over beach cusps spanning a fixed length $|\beta_{01}^{+}\beta_{12}^{-}|^{1/2}L = 10.0$, for different detuning $k_0|\beta_{01}^{+}\beta_{12}^{-}|^{-1/2}|\Omega|/\omega = 0$ (*a*), 1.5 (*b*), and 3.0 (*c*). The incident wave is mode 0.

for a mode-2 incident wave, where

$$D = a_0 g\left[2i\omega(|\beta_{01}^{+}|^2 - |\beta_{12}^{-}|^2\cos RL)\right]^{-1}, \quad R = \left(|\beta_{01}^{+}|^2 - |\beta_{12}^{-}|^2\right)^{1/2} > 0, \tag{4.17}$$

$$r_{10} = (3^{1/2} - 1)^{1/2}, \quad r_{20} = (2 - 3^{1/2})^{1/2}, \quad r_{21} = [(3^{1/2} - 1)/2]^{1/2}. \tag{4.18}$$

All multi-wave solutions with perfect tuning $\Omega = 0$ are periodic. From (4.14)–(4.16), it can be shown that the following reciprocal property holds: $F_{10}^{+}(L) = F_{01}^{+}(L)$, $F_{20}^{-}(0) = F_{02}^{-}(0)$, and $F_{21}^{-}(0) = F_{12}^{-}(0)$.

Scattering by beach cusp topography given by $\epsilon h_1(x, y) = a_c e^{-\pi x/\lambda_c}\cos(2\pi y/\lambda_c)$ is considered first. For this particular topographic perturbation (corresponding to $p = (3 - \sqrt{3})/4, q = 0$ in (4.1CG)), the coupling coefficients are $\beta_{01}^{+}/k_0 = 0.1036$ and $\beta_{12}^{-}/k_0 = 0.0163$, and the Ω separating regions of different roots of the characteristic equation (4.11) are $k_0|\beta_{01}^{+}\beta_{12}^{-}|^{-1/2}\Omega_1/\omega = 1.045$ and $k_0|\beta_{01}^{+}\beta_{12}^{-}|^{-1/2}\Omega_2/\omega = 1.810$. Over a moderately short scattering region (e.g. $|\beta_{01}^{+}\beta_{12}^{-}|^{1/2}L \leqslant 1.0$), backscattering is weak regardless of the magnitude of the detuning and the mode number of the incident wave. For a mode-0 or mode-1 incident wave, energy exchange mostly occurs between two forward propagating mode-0 and mode-1 waves; for a mode-2 incident wave, only a small portion (less than 10%) of the incident wave energy is transfered to the two backscattered (mode-0 and mode-1) edge waves (not shown). Over a long beach

cusp region, the variations of the normalized energy fluxes depend on the frequency detuning $|\Omega|$. The variations of energy fluxes over a long cusped region ($|\beta_{01}^{+}\beta_{12}^{-}|^{1/2}L = 10.0$) for Ω in each detuning region $0 \leqslant |\Omega| < \Omega_1$, $\Omega_1 < |\Omega| < \Omega_2$, and $|\Omega| > \Omega_2$ with a mode-0 incident wave are shown in figure 2. When $0 \leqslant |\Omega| < \Omega_1$ (figure 2*a*), backscatter is insignificant, and the wave field over the perturbed depth is dominated by nearly complete energy exchange between the incident mode-0 edge wave and the forward scattered mode-1 edge wave. Note that the incident wave amplitude is slightly amplified at some locations inside the undulating region. In the region $\Omega_1 < |\Omega| < \Omega_2$ (figure 2*b*), the normalized energy flux of the backscattered mode-2 wave F_{20}^{-} near the upwave edge $Y = 0$ reaches 0.3; both F_{00}^{+} and F_{10}^{+} oscillatorily approach constants as Y increases. In the region $|\Omega| > \Omega_2$ (figure 2*c*), backscattering becomes insignificant again; the amplitudes of both forward propagating waves oscillate over the perturbed bathymetry with partial exchange of energy. As the detuning further increases (not shown), both the magnitude and wavelength of the forward amplitude oscillations decrease, indicating the weakening influence of the undulating region.

The variations of normalized energy fluxes outside a long undulating region as a function of normalized detuning are shown in figure 3 for a mode-0 incident wave. With small detuning $0 \leqslant |\Omega| < \Omega_1$ (i.e. $k_0|\beta_{01}^{+}\beta_{12}^{-}|^{-1/2}|\Omega|/\omega < 1.045$) that includes the perfect tuning case, backscattering into the mode-2 wave is insignificant for all region lengths, and transmission of the incident mode-0 wave is nearly complete for the particular value $|\beta_{01}^{+}\beta_{12}^{-}|^{1/2}L = 10.0$ in figure 3(*a*). However, transmission depends periodically on the region length (as expected from figure 2*a*) and can be small for different normalized lengths (e.g. $|\beta_{01}^{+}\beta_{12}^{-}|^{1/2}L = 9.5$ in figure 3*b*). With increased detuning ($\Omega_1 < |\Omega| < \Omega_2$), the results over a long undulating region are less sensitive to the region length. Backscattering of the incident mode-0 wave energy flux to mode 2 is maximum (about 40%, dashed lines in figure 3) with detuning in this region (i.e. $1.045 < k_0|\beta_{01}^{+}\beta_{12}^{-}|^{-1/2}|\Omega|/\omega < 1.810$). As detuning further increases ($|\Omega| > \Omega_2$), backscattering again weakens and most of the incident wave energy reaches the downwave region $Y \geqslant L$ as mode-1 and/or the original mode-0 incident edge wave.

Over the same perturbed region, the variations of the normalized energy fluxes of a mode-1 incident wave (F_{11}^{+}), forward scattered mode-0 wave (F_{01}^{+}), and backscattered mode-2 wave (F_{21}^{-}) are similar to those of the corresponding energy fluxes for a mode-0 incident wave (F_{00}^{+}, F_{10}^{+}, and F_{20}^{-}), respectively, except that more incident wave energy flux is backscattered into mode-2 with a mode-1 incident wave (as much as 70%) than with a mode-0 incident wave (40%) in the region $\Omega_1 < |\Omega| < \Omega_2$ (cf. dashed lines in figures 3*a* and 4 for $1.045 < k_0|\beta_{01}^{+}\beta_{12}^{-}|^{-1/2}|\Omega|/\omega < 1.810$). Note that $F_{01}^{+}(L)$ is identical to $F_{10}^{+}(L)$ for arbitrary detuning Ω (cf. solid line in figure 4 with dotted line in figure 3*a*).

With a mode-2 incident wave, the scattered mode-0 and mode-1 waves are both backward propagating, in contrast to the cases of a mode-0 or mode-1 incident wave where one scattered wave is forward propagating. Consequently, the variations of energy fluxes over the same undulating region with a mode-2 incident wave differ from those with a mode-0 or mode-1 incident wave. For instance, results over a long corrugated region with a mode-2 incident wave are not sensitive to the region length L, in contrast to a mode-0 or mode-1 incident wave. Over a corrugated region of any length, the energy fluxes of both mode-0 and mode-1 backscattered waves are small when $0 \leqslant |\Omega| < \Omega_1$ or $|\Omega| > \Omega_2$, and even a long undulating region has little effect on the mode-2 incident wave (figure 5). However, when $\Omega_1 < |\Omega| < \Omega_2$, F_{02}^{-}, F_{12}^{-}, and F_{22}^{+} monotonically decrease during propagation over a long undulating region (contrast figure 6 with 2*b*). Almost no energy reaches the downwave end of the

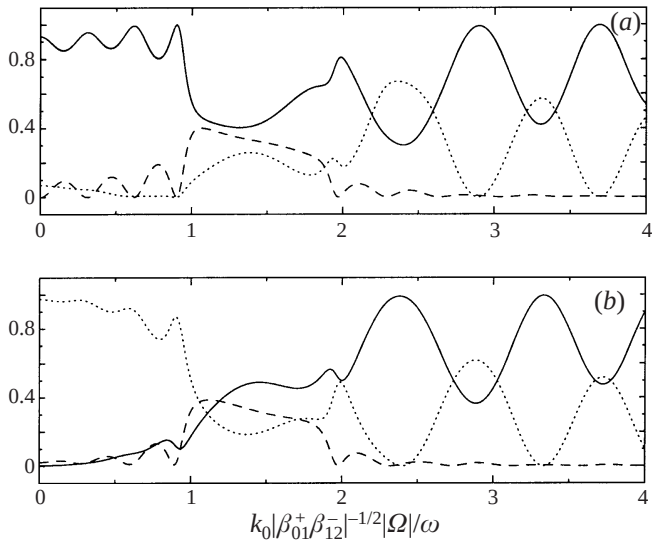

FIGURE 3. Variations of energy fluxes at the edges of the undulating region $Y = 0, L$ (——, $F_{00}^+(L)$; · · · ·, $F_{10}^+(L)$; and - - -, $F_{20}^-(0)$) versus the detuning $k_0|\beta_{01}^+\beta_{12}^-|^{-1/2}|\Omega|/\omega$ for region length $|\beta_{01}^+\beta_{12}^-|^{1/2}L = 10.0$ (*a*) and 9.5 (*b*). $F_{00}^+(L) = 1$ corresponds to complete transmission of the mode-0 incident wave.

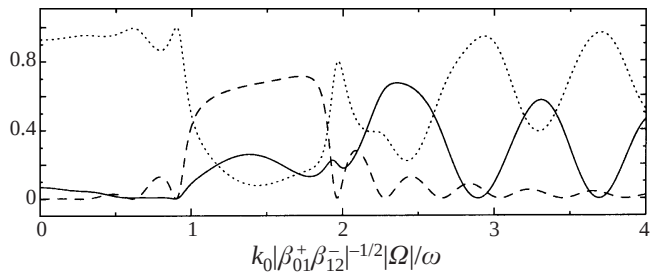

FIGURE 4. Variations of energy fluxes (——, $F_{01}^+(L)$; · · · ·, $F_{11}^+(L)$; and - - -, $F_{21}^-(0)$) versus the detuning $k_0|\beta_{01}^+\beta_{12}^-|^{-1/2}|\Omega|/\omega$ with fixed $|\beta_{01}^+\beta_{12}^-|^{1/2}L = 10.0$. $F_{11}^+(L) = 1$ corresponds to complete transmission of the mode-1 incident wave.

perturbed bathymetry, resulting in nearly complete backscattering (i.e. $F_{22}^+(L) \approx 0$ and $F_{02}^-(0)+F_{12}^-(0) \approx 1$ in figures 5 and 6). More incident wave energy flux is backscattered to mode 1 than to mode 0 in this detuning region (cf. dotted line with solid line in figures 5 and 6). The reciprocal property holds for all detuning values: $F_{02}^-(0) = F_{20}^-(0)$ and $F_{12}^-(0) = F_{21}^-(0)$ (cf. solid line in figure 5 with dashed line in figure 3*a* and dotted line in figure 5 with dashed line in figure 4).

The multi-wave scattering results presented above are not sensitive to the particular assumed cross-shore variation of the depth perturbation. Almost identical results are obtained for beach cusps with a range of plausible p and q values in the more general cusp perturbation (4.1CG) discussed in CG, because the ratio $|\beta_{01}^+/\beta_{12}^-|$, the only parameter determining the scaled results plotted in figures 2–6, is almost the same. For bathymetry roughly resembling the crescentic bars observed at Duck, North Carolina (discussed in CG), the variations of normalized energy fluxes are similar to the corresponding results above for beach cusps.

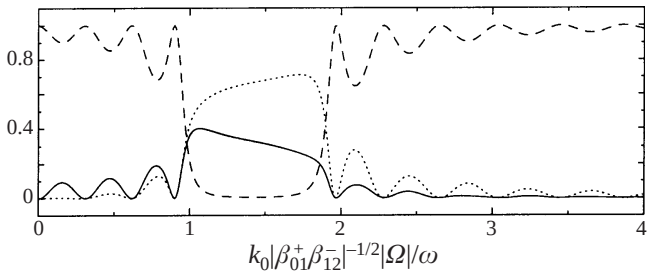

FIGURE 5. Variations of energy fluxes (——, $F_{02}^-(0)$; ····, $F_{12}^-(0)$; and - - -, $F_{22}^+(L)$) versus the detuning $k_0|\beta_{01}^+\beta_{12}^-|^{-1/2}|\Omega|/\omega$ with fixed $|\beta_{01}^+\beta_{12}^-|^{1/2}L = 10.0$. $F_{22}^+(L) = 1$ corresponds to complete transmission of the mode-2 incident wave.

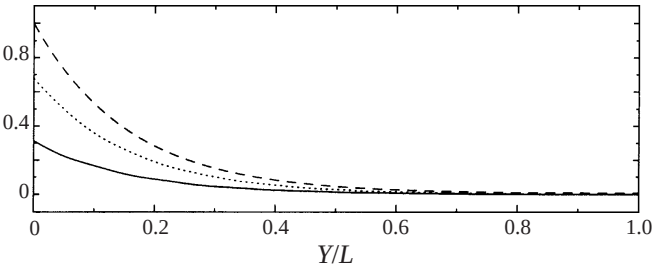

FIGURE 6. Spatial variations of energy fluxes (——, F_{02}^-; ····, F_{12}^-; and - - -, F_{22}^+) for multi-wave scattering at $\theta = \pi/12$ over beach cusps spanning a fixed length $|\beta_{01}^+\beta_{12}^-|^{1/2}L = 10.0$ for a mode-2 incident wave with detuning $k_0|\beta_{01}^+\beta_{12}^-|^{-1/2}|\Omega|/\omega = 1.5$.

5. Discussion

Simple corrections to the shallow water evolution equations accounting for the differences in the exact and shallow water dispersion relations are given in § 3 for single-wave scattering and in § 4 for multi-wave scattering involving mode-0 and mode-1 edge waves. The size of these corrections is proportional to $\hat{\theta}^2 = \theta^2/\epsilon$. For sufficiently large $\hat{\theta}^2$, the corrections may change the character of the incident and scattered wave fields. For resonant scattering by beach cusps (4.1CG) and crescentic bars (4.5CG), the ordering parameter $\epsilon = a_c k_0/\tan\theta$, where a_c is the amplitude of the undulations. It follows that $\hat{\theta}^2 = \theta^2/\epsilon = \theta^2 \tan\theta/a_c k_0 \approx \theta^3/a_c k_0$.

CG applied the shallow water scattering theory to undulating bathymetry with shapes and dimensions roughly resembling field observations of cusps at Parramore Island and crescentic bars at Duck Beach. These topographies are considered here. The first row in table 1 gives the normalized finite-slope corrections $\Delta K/|\beta_{nm}^-| = [2 + (2n + 1)(2m + 1)]\hat{\theta}^2 k_t/12|\beta_{nm}^-|$ (from (3.20)) for single-wave backscattering B_{00}, B_{01}, B_{02}, and B_{12}, and $k_0|\beta_{01}^+\beta_{11}^-|^{-1/2}\hat{\theta}^2$ for multi-wave scattering M_{01}, of a perfectly tuned (based on the shallow water dispersion relation) incident wave propagating over Parramore beach cusps $\epsilon h_1(x, y) = a_c e^{-\pi x/\lambda_c}\cos(2\pi y/\lambda_c)$. The first row in table 2 gives similar results for the Duck crescentic bar (4.5CG). In the single-wave backscattering case, the threshold value $\Delta K/|\beta_{nm}^-| = 1$ corresponds to a change from exactly resonant scattering with exponentially decaying amplitudes over the perturbed region to supercritical scattering with oscillatory amplitudes. In the multi-wave scattering case, the threshold value of $k_0|\beta_{01}^+\beta_{11}^-|^{-1/2}\hat{\theta}^2$ corresponding to a change from nearly complete backscattering to dominant forward scattering (cf. figure 1*a* with 1*b–d*) is

	B_{00}	B_{01}	B_{02}	B_{12}		M_{01}
$\Delta K/\lvert\beta_{nm}^{-}\rvert$	0.031	0.104	0.216	0.542	$k_0\lvert\beta_{01}^{+}\beta_{11}^{-}\rvert^{-1/2}\hat{\theta}^2$	0.281
θ_c(rad)	0.222	0.149	0.117	0.086	θ_c (rad)	0.087

TABLE 1. Finite-slope effect on low-mode edge wave scattering by beach cusps at Parramore Island. Values of the normalized finite-slope corrections ($\Delta K/\lvert\beta_{nm}^{-}\rvert$ and $k_0\lvert\beta_{01}^{+}\beta_{11}^{-}\rvert^{-1/2}\hat{\theta}^2$) and critical slope angle (θ_c) are listed. The cusp dimensions are $\lambda_c = 20$ m, $\tan\theta = 0.07$, and $a_c = 0.035$ m (from Guza & Bowen 1981).

	B_{00}	B_{01}	B_{02}	B_{12}		M_{01}
$\Delta K/\lvert\beta_{nm}^{-}\rvert$	0.007	0.034	0.109	0.067	$k_0\lvert\beta_{01}^{+}\beta_{11}^{-}\rvert^{-1/2}\hat{\theta}^2$	0.052
θ_c (rad)	0.157	0.092	0.063	0.074	θ_c (rad)	0.065

TABLE 2. Finite-slope effect on low-mode edge wave scattering by Duck crescentic sandbar (4.5, in Chen & Guza 1998) with $\lambda_c = 250$ m, $\tan\theta = 0.03$, $a_c = 0.5$ m, $b = 50$ m, and $c = 0.0314$ m^{-1}.

0.545 for the Parramore beach cusps and 0.521 for the Duck crescentic bar. The beach angles θ_c corresponding to $\Delta K/\lvert\beta_{nm}^{-}\rvert = 1$ and $k_0\lvert\beta_{01}^{+}\beta_{11}^{-}\rvert^{-1/2}\hat{\theta}^2 = 0.545$ or 0.521 are given in the second row of the tables. For single-wave backscattering, $\Delta K/\lvert\beta_{nm}^{-}\rvert$ generally increases and θ_c decreases as mode numbers increase, consistent with the expectation that finite-slope corrections increase in importance as the mode number increases. For all cases considered, $\Delta K/\lvert\beta_{nm}^{-}\rvert$ and $k_0\lvert\beta_{01}^{+}\beta_{11}^{-}\rvert^{-1/2}\hat{\theta}^2$ are less than their threshold values, and θ_c is greater than the actual beach slope angle. Thus, the shallow water results given by CG are at least qualitatively correct.

This research was supported by the Mellon Foundation and the Office of Naval Research (Coastal Dynamics).

REFERENCES

CHEN, Y. & GUZA, R. T. 1998 Resonant scattering of edge waves by longshore periodic topography. *J. Fluid Mech.* **369**, 91–123 (referred to herein as CG).

GUZA, R. T. & BOWEN, A. J. 1981 On the amplitude of beach cusps. *J. Geophys. Res.* **86**, 4125–4132.

HEATHERSHAW, A. D. 1982 Seabed-wave resonance and sandbar growth. *Nature* **296**, 343–345.

MEI, C. C. 1985 Resonant reflection of surface water waves by periodic sandbars. *J. Fluid Mech.* **152**, 315–335.

URSELL, F. 1952 Edge waves on a sloping beach. *Proc. R. Soc. Lond.* A **214**, 79–97.